Medical imaging by Fluorescent X-ray CT: Its preliminary clinical evaluation

Tohoru Takeda, Tsutomu Zeniya, Jin Wu, Quanwen Yu, Thet-Thet-Lwin, Yoshinori Tsuchiya, Donepudi V. Rao, Tetsuya Yuasa*, Toru Yashiro, F. Avraham Dilmanian**, Yuji Itai and Takao Akatsuka*

Institute of Clinical Medicine, University of Tsukuba. Tsukuba-shi, Ibaraki 305-8575 Japan
*Faculty of Engineering, Yamagata University. Yonezawa-shi, Yamagata 992-8510 Japan
**Medical Department, Brookhaven National Laboratory, Upton, NY 11973 USA

Abstract

Fluorescent x-ray CT (FXCT) with synchrotron radiation (SR) is being developed to detect the very low concentration of specific elements. The endogenous iodine of the human thyroid and the non-radioactive iodine labeled BMIPP in myocardium were imaged by FXCT. FXCT system consists of a silicon (111) double crystal monochromator, an x-ray slit, a scanning table for object positioning, a fluorescent x-ray detector, and a transmission x-ray detector. Monochromatic x-ray with 37 keV energy was collimated into a pencil beam (from 1 mm to 0.025 mm).

FXCT clearly imaged endogenous iodine of thyroid and iodine labeled BMIPP in myocardium, whereas transmission x-ray CT could not demonstrate iodine. The distribution of iodine was heterogeneous within thyroid cancer, and its concentration was lower than that of normal thyroid. Distribution of BMIPP in normal rat myocardium was almost homogeneous, however reduced uptake was slightly shown in ischemic region. FXCT is a highly sensitive imaging modality to detect very low concentration of specific element and will be applied to reveal endogenous iodine distribution in thyroid and to use tracer study with various kinds of labeled material.

KEYWORDS: fluorescent x-ray CT, synchrotron radiation, thyroid imaging, myocardial imaging

1. INTRODUCTION

Fluorescent x-ray technique used in the planar mode is one of the most sensitive methods for elemental analysis of sample [1]. This method is applied to assess various kinds of biomedical object, i.e., the intoxication of Hg [2, 3], distribution of cis-Pt in cancer therapy [4, 5], distribution of Cu, Se, and Zn of renal cancer [6], metal-ion release from a hip replacement prosthesis [7], and metal deposition of Parkinson disease. It can evaluate very low contents in the order of picograms per gram of specific elements. However, the method requires the specimen to be cut into thin slices and scanned

Developments in X-Ray Tomography III, Ulrich Bonse, Editor,
Proceedings of SPIE Vol. 4503 (2002) © 2002 SPIE · 0277-786X/02/$15.00

with a beam perpendicular to its surface.

Transmission x-ray computed tomography (TXCT), which demonstrates the inside morphological structures of objects, dose not require the specific preparation of a specimen described above. However, its minimal detectable concentration of specific element was limited in the order of tens of micro-grams per gram even used the excellent properties of synchrotron radiation (SR) [8-12] and K-edge energy subtraction is required to select the specific element. Then, we have developed the fluorescent x-ray computed tomography (FXCT) to detect very low content of elements for biomedical use as the analog of x-ray CT.

2. MEDICAL APPLICATION OF FXCT

FXCT can be visualized from two perspectives; one is the micro-imaging of the pathological specimens and another one is the imaging of the living objects.

2-1. Micro-FXCT

Micro-FXCT imaging of the pathological objects is also being developed to detect the distribution of specific elements at the spatial resolution of micrometer order. However, micro-FXCT imaging of relatively low atomic number elements as Cu, Zn and As, might be inadequate because the excited fluorescent x-rays of these elements are absorbed by object itself, and detailed comparison with pathological picture is required.

We are planning to image the high atomic number elements as iodine, Pt and Gadolinium et. al. Especially the imaging of iodine containing object is thought to be most adequate targets for micro-FXCT. First target is the detection of iodine included within thyroid follicle as the colloid of thyroid hormone. Quantitative evaluation of iodine distribution in thyroid specimens is used to predict the therapoietic effect of ^{131}I for thyroid cancer or hyperthyroidism [13]. Approach with FXCT can easily measure the absolute content of iodine comparing to neutron activation method, and improves the cutting problem of specimens for optical microscopy because the colloid was sometimes lost from follicle.

Secondly the distribution of iodine labeled tracer elements comparable to the autoradiogram might be detected in this method [14]. For example, single photon emission computed tomogram (SPECT) was used to assess the perfusion, metabolism, apoptosis and receptor condition of various organs clinically. However, spatial resolution of SPECT does not allow the detailed measurement of the biological distribution of new radionuclide agents that are being synthesized and should be evaluated by animal experiments for clinical use. We applied FXCT to image rat myocardium using 15-(p-iodophenyl)-3-methlpentadecanoic acid (BMIPP) labeled with non-radioactive.

2-2. FXCT for live object

FXCT is being developed to detect non-radioactive contrast agents (high Z-elements) at concentrations comparable to those of radionuclides used in single photon emission computed tomography (SPECT) [15]. So FXCT might be the only analogous method to SPECT. The spatial resolution of the SPECT system, about 8 x 8 x 8 mm^3, is presently not good for

detailed image analysis of human study. In contrast, positron emission tomography (PET) affords relatively excellent spatial resolution of about 4 x 4 x 4 mm^3 comparing to SPECT, but the synthetic system of drug and cyclotron are indispensable to perform PET study [16]. FXCT has the possibility to image at the spatial resolution of PET resembling to the approaches of SPECT without the use of non-radioactive elements. The sensitivity of FXCT is about 77 times better than that of the TXCT in the 3-cm diameter phantom [17].

3. DEVELOPMENT OF FLUORESCENT X-RAY TOMOGRAPHY AND CT WITH SR

Micro-tomography with SR was first implemented to detect iron in the head of a bee in 1987 [18]. Fluorescent x-ray tomography with SR then followed to detect about 200 ng iodine in a volume of 4 mm^3 [16, 19], compared to the limit of 5 mg iodine in a volume of 16.3 mm^3 using x-ray tubes [20].

In the tomographic approach, the detection limit of excited fluorescent x-rays worsens as the requirement for better spatial resolution in the CT image is imposed. However, our FXCT has a highly efficient system for detecting the excited fluorescent x-rays compared to the tomographic approaches since the FXCT system does not require intense collimation in detection site. As a result, our FXCT can also reduce the x-ray exposure and the related risks to the subjects. Such FXCT system has been found to enable an efficient detection of fluorescent x-rays using phantom studies in 1996 [15]. FXCT employing 37-keV monochromatic synchrotron x-rays and a parallel collimator, could detect about 60 ng iodine in a volume of 1 mm^3 [21]. Theoretical consideration of FXCT was done in 1992 by Hogan [22].

For the first biomedical application, FXCT was applied to depict the cross sectional distribution of iodine within the thyroid gland, in vitro, at the spatial resolution of 1 mm [13, 23] and less than 0.2-mm [24, 25]. In addition, images with about 0.006 mm spatial resolution was also obtained by FXCT [26, 27].

Here, we present micro FXCT images of the human thyroid gland and rat myocardium labeled by non-radioactive BMIPP.

4. METHODS AND MATERIALS

The experiment was carried out at the bending-magnet beam line BLNE-5A of the Tristan accumulation ring (6.5 GeV, 10 - 30 mA) in Tsukuba, Japan. Using an ion chamber, the photon flux rate in front of the object was measured to be approximately 7 x 10^7 photons/mm^2/sec at a beam current of 30 mA.

4.1 FXCT system

The FXCT system consisted of a silicon (111) double crystal monochromator, a pin diode, an x-ray slit system, a scanning table for subject positioning, a fluorescent x-ray detector with its x-ray collimator, and a transmission x-ray detector with its x-ray shutter (Fig.1). The fluorescent x-ray detector was positioned perpendicular to the incident monochromatic x-ray beam to reduce the amount of stray radiation reaching the detector.

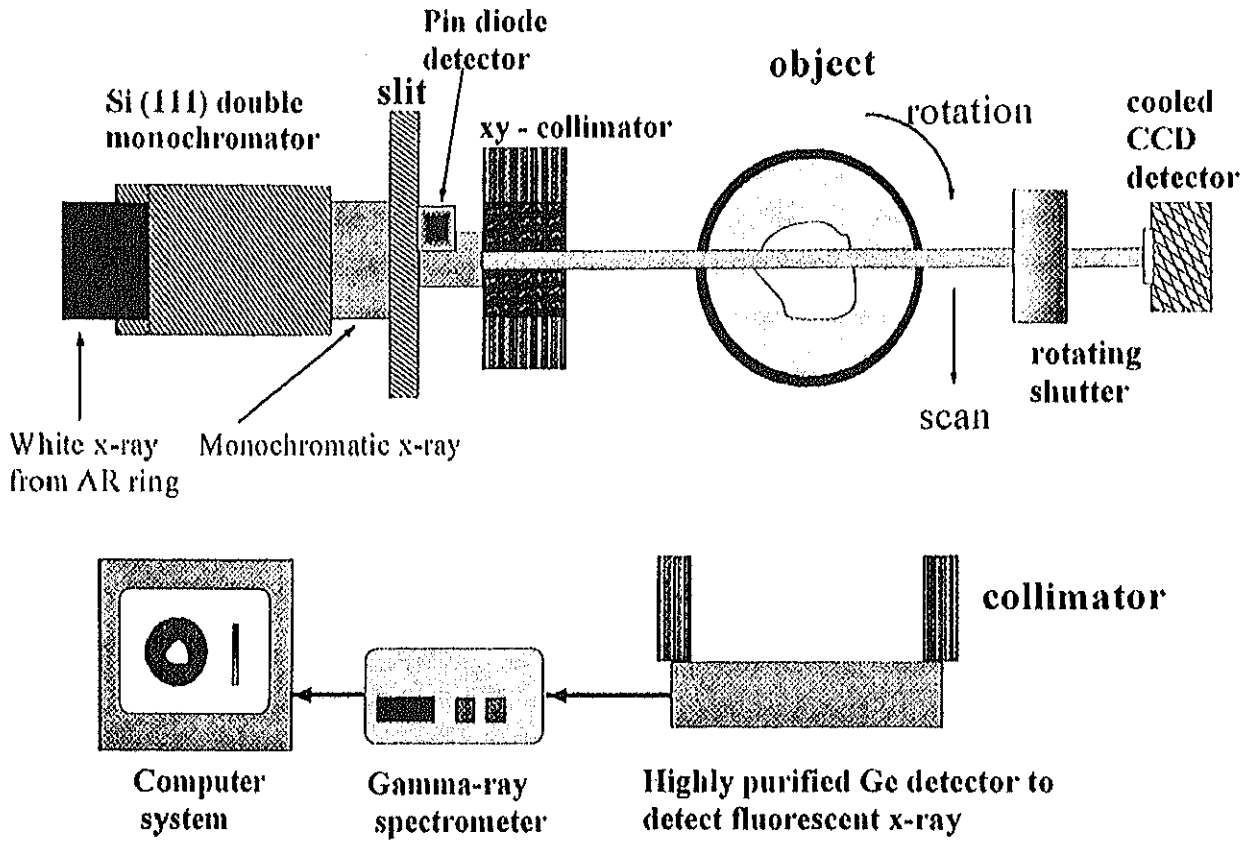

Fig. 1 Schematic diagram of fluorescent x-ray CT

4.2 Fluorescent x-ray detector

Fluorescent x-rays, which are emitted isotropically from the subject along the path of the incident x-ray beam, were detected by a highly purity germanium (HPGe; LO-AXTH Series, EG&G Ortec Ltd., USA) detector with digital gamma-ray spectrometer (DSPEC spectrum master, EG&G Ortec Ltd) operating in the photon-counting mode. The energy resolution was about 700 eV with a shaping time 2 μ s at 30 keV [28]. The active detection of HPGe was 51.2-mm in diameter.

4.3 Transmission x-ray detector

The transmission x-ray detector was fiber-optically interface x-ray CCD camera cooled by a Peltier thermoelectric cooling (- 35 °C) (Princeton Instruments Ltd., USA). This x-ray CCD camera had 1240 x 1024 pixels and its pixel size was a 22.5 μ m x 22.5 μ m. Data was digitized in 16-bit A/D converter. The dynamic range of this detector was about 60000:1. An x-ray shutter was set in front of x-ray CCD camera to prevent radiation damage.

4.4 Pin diode

The monochromatic x-ray intensity declined exponentially owing to the decrease of the ring current, hence the change of monochromatic x-ray intensity was measured by PIN diode operated in the current integration mode by a pico-ammeter

(486, Keithley Ltd., USA). The measured data was digitized by a 16 bit analog-to-digital converter (BNC 2090, National Instruments Ltd., USA) and read into a PC (Aptiva, IBM Ltd., USA).

4.5 System control

In the fluorescent x-ray CT system, a PC (Presario 5000, Compaq Ltd., USA) controlled a pulse motor controller (AS-NET3, Sigma Koki Ltd., Japan). The pulse motor controller controlled the translation-rotation table and rotating x-ray shutter. An automated data-collection procedure was developed using "Labview" (National Instruments Ltd., USA).

4.6 Image reconstruction

The net counts under the characteristic fluorescent Kα x-ray spectral lines at each projection were used to generate a CT projection. The data acquisition time of x-ray CCD camera was 0.2-s at each scanning step. Transmission x-ray CT images were reconstructed using a filtered back-projection method. The x-ray fluorescent data were corrected for the attenuation of the incident beam and the emitted fluorescent x-ray, using the attenuation information from the transmission x-ray CT image data. FXCT images were reconstructed from a system of algebraic equations representing the attenuation process, using a least-squares method which is based on singular value decomposition (ALS) [29].

4.7 Experimental condition of FXCT: X-ray energy selection and the formulation of pencil beam

The white x-ray beam was monochromatized at 37.0 keV using a silicon double crystals monochromator, and the size of incident monochromatic x-ray beam was 65-mm in width by 3-mm in height. To make a pencil beam, the incident monochromatic x-ray was collimated into a 1.0 mm x 1.0 mm beam to a 0.025 mm x 0.025 mm beam (horizontal and vertical direction, respectively) using a tantalum x-ray slit (Kohzu Ltd., Japan).

Table 1 Condition of data acquisition

	spatial resolution (mm)	distance HPGe-specimen (mm)	translational step (mm)	rotational step over 180 (degree)	Time (sec)
Thyroid	1	200	1	3	5
	0.1	45	0.1	1.2	5
	0.025	20	0.025	1.2	5
Heart	0.2	45	0.2	2	5
	0.1	45	0.1	1.5	10

4.8 Object

The objects were a 10-mm-diameter acrylic phantoms with three 3-mm-holes filled with iodine solutions at different concentrations, rat myocardium labeled BMIPP, and human thyroid fixed in 10% formalin. Phantom images were obtained

to achieve a quantitative estimation for the iodine content of the thyroid.

Non-radioactive iodine labeled BMIPP (iodine content of total injection dose: 0.1 mg) which reveals the metabolic state of fatty acid, was injected into living rat heart under the Langendorf procedure. The heart labeled with BMIPP was soon fixed by formalin and 10 mm in diameter of heart sample was imaged by FXCT.

The present experiment was approved by the Medical Committee for the Use of Animals in Research of the University of Tsukuba, and it conformed to the guidelines of the American Physiological Society.

5. RESULTS AND DISCUSSION

5.1 Phantom experiment

In the 10-mm diameter, 3-hole, phantom image, the 0.005 mg/ml iodine solution could be visualized at 0.1 x 0.1 mm^2 spatial resolution with 0.1 mm slice thickness by FXCT. Observation of the 0.005 mg/ml iodine solution indicated that the excited iodine content in the measured voxel is about 5 pg (0.005 mg/ml x 1 x 10^{-6} ml). A linear correlation was observed between the iodine concentration and fluorescent x-ray counts in the phantom study (Fig.2). Then, FXCT may be used to detect iodine at low concentration quantitatively.

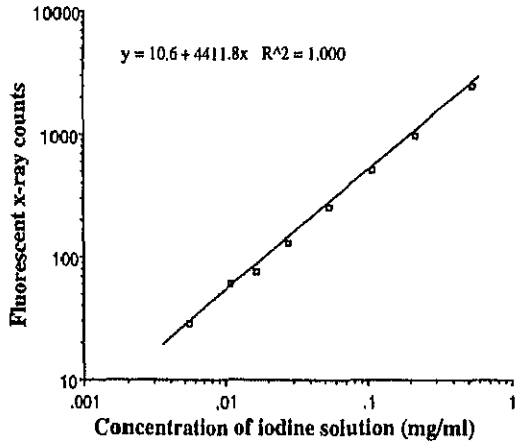

Fig.2 The relationship between fluorescent x-ray counts and iodine concentration

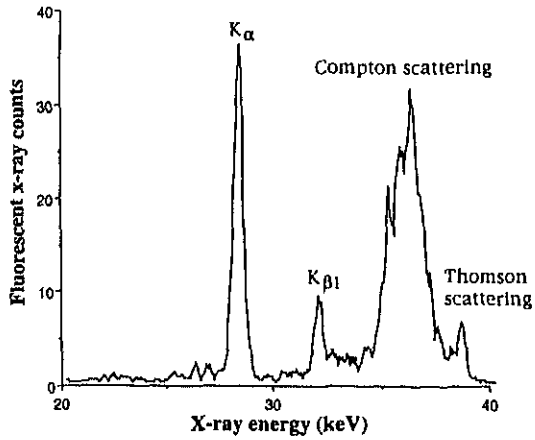

Fig.3 An energy spectrum obtained the human thyroid gland at 0.025mm spatial resolution by the fluorescent x-ray CT.

5.2 FXCT image of thyroid specimens

The Kα and Kβ1 fluorescent x-ray lines of iodine within the normal thyroid gland, together with the background of Compton scattering and Coherent scattering, are shown at 0.025-mm in-plane spatial resolution and 0.025-mm slice thickness (Fig.3). The distribution of iodine included within thyroid follicle as the colloid of thyroid hormone was clearly visualized by FXCT (Fig.4). The heterogeneous iodine distribution by FXCT lead to inhomogeneous distribution of the iodine, vessel structures and connective tissues within the thyroid gland. Since the transmission x-ray CT cannot distinguish the histopathological structures of soft tissue at the order of micrometer spatial resolution (due to the poor signal to noise

ratio). A combined analysis using both micro FXCT and conventional pathological image is necessary to differentiate various organs or tissues not including iodine such as vessels and connective tissues. However, 3D reconstruction of FXCT image might be helpful to distinguish the vessel and connective tissue from thyroid follicle because these structures have specific network structures

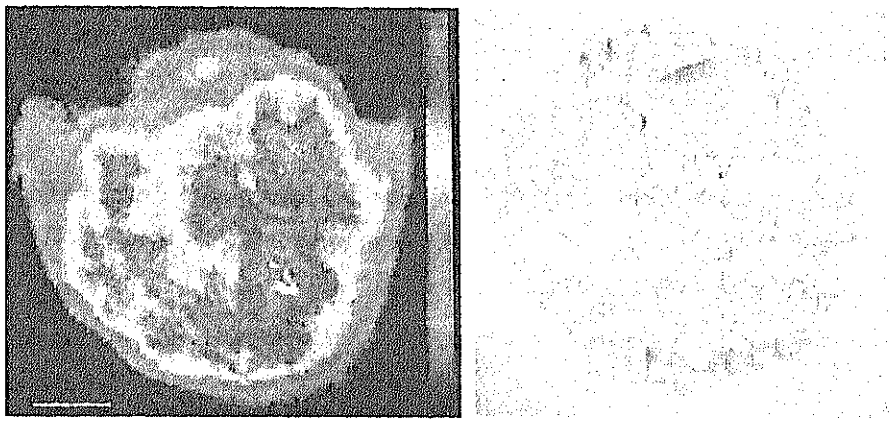

Fig.4 Fluorescent x-ray CT image of normal thyroid gland at 0.025 mm spatial resolution and pathological picture. Heterogeneous distribution of iodine within the human thyroid gland was revealed.

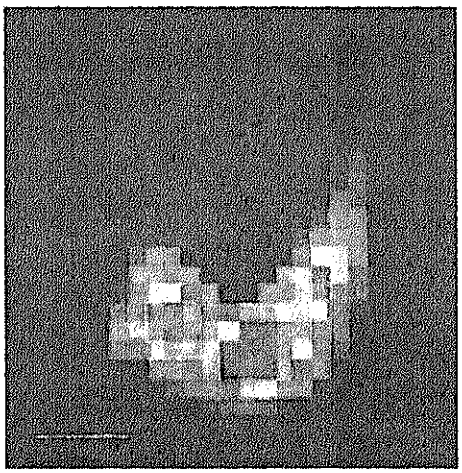

Fig.5 Fluorescent x-ray CT image of thyroid cancer at 1-mm spatial resolution.

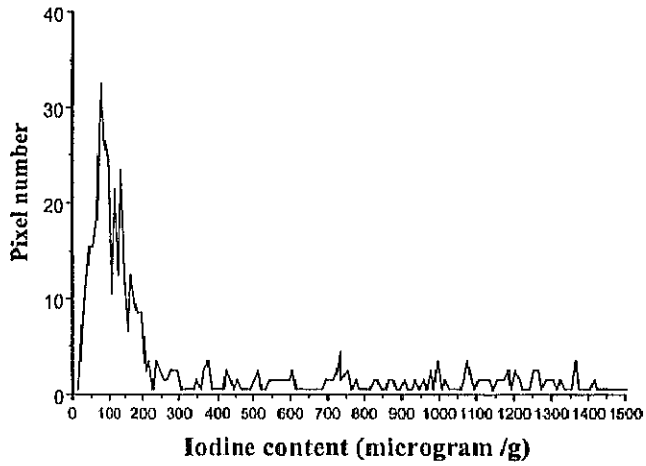

Fig.6 The relationship between pixel number and iodine concentration in thyroid cancer.

In thyroid cancer, cancer lesion was shown as defect (Fig.5) because the content of iodine in cancer was small amounts comparing to normal thyroid [30-32]. Quantitative analysis revealed the concentration of iodine within cancer (Fig.6) was less than 0.2 mg/g. As the accumulation dose of ^{131}I in pathological targets will be estimated by FXCT, quantitative evaluation of iodine will be useful to predict the effectiveness of ^{131}I therapy for thyroid cancer and hyperthyroidism. In addition, FXCT method is much easier than the neutron activation analysis.

5.3 FXCT image of rat myocardium

Spectrum of fluorescent Kα line and Compton scattering was detected by FXCT. The content of iodine in myocardium was estimated to be about 0.01 mg/g from the fluorescent Kα counts. Using Kα line, FXCT image could clearly reveal the distribution of ^{127}I-BMIPP within myocardium both at 0.1 mm and 0.2 mm in-plane spatial resolution and 0.1 mm and 0.2 mm slice thickness (Fig.7). The image quality reconstructed by an algebraic reconstruction method including the attenuation correction (ALS) was better than that by a filtered back projection (FBP) procedure without absorption correction. A part of cardiac muscle showed reduced uptake, this might have been caused by myocardial ischemia produced with Langendorf procedure.

Thus, FXCT will be used to evaluate the distribution of labeling elements resembled to the autoradiogram or SPECT study with radionuclide agents.

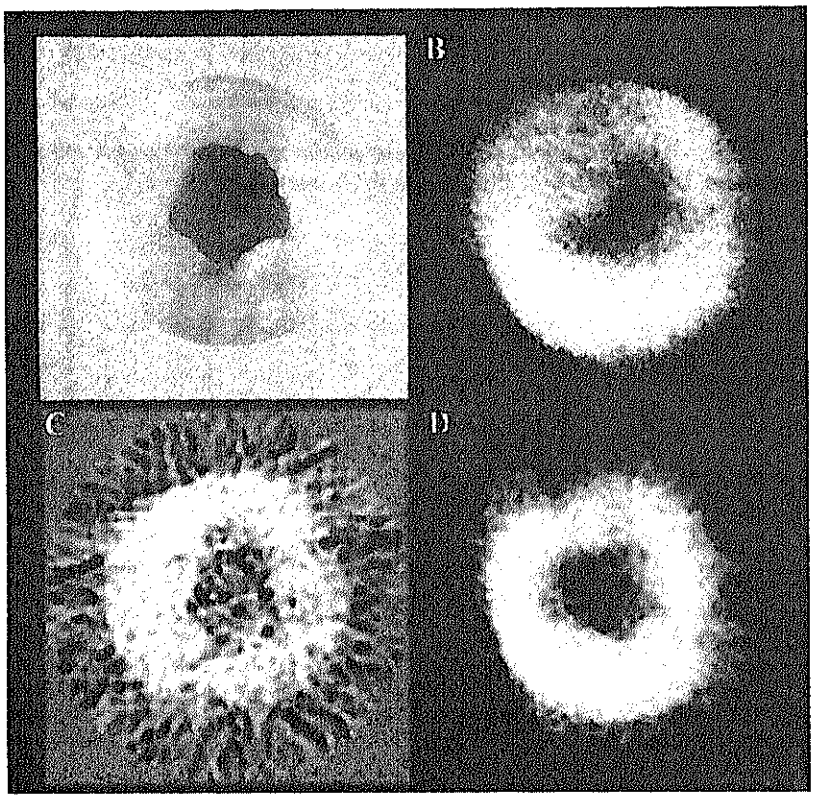

Fig.7 Fluorescent x-ray CT image of rat myocardium labeled by BMIPP.
A: FXCT with 0.1 mm spatial resolution (ALS),
B: pathological picture.
C & D: FXCT with 0.2 mm spatial resolution (FBP & ALS).

5.4 Present limitations and future plans

In our FXCT system, the obtainable spatial resolution was limited 0.025 mm owing to the precision of mechanical system. Now a new system is being constructed to obtain a few micrometer spatial resolution. Imaging for micrometer spatial resolution requires very long data acquisition time because the scan number of translation and rotation increase significantly. Using a HPGe detector with DSPEC electronics, the count-rate capability of the detector has improved 6-fold as compared to the previous detector system [28]. However, new FXCT system is being designed to acquire image data at 4-times faster than present system; it will use two detectors positioned symmetrically on both sides of the subject, and new

electronics with much higher count-rate capability. In addition, Tristan AR ring is now on renewal. The storage current will be 70 mA (present 30 mA) and the life becomes more than 12 hr (present 2 – 3 hr for adequate measurement).

6. CONCLUSION

The high spatial resolution and the high sensitivity of FXCT indicate the potential of this new imaging modality to use various research applications in vivo animal and in vitro specimen studies

ACKNOWLEDGEMENT

We would like to thank Mr. Yasuhiro Hasegawa for their help with FXCT, Kazuyuki Hyodo, PhD, for their technical supports at the Photon Factory and the Tristan AR ring and Mr. K. Kobayashi for his preparation of experimental apparatus. This research was partially supported by a Grant-in-aid for Scientific Research (#10557084, 12307018 and 13470178) from the Japanese Ministry of Education, Science and Culture, and was performed under the auspices of the National Laboratory for High Energy Physics (Proposal : 99G124).

REFERENCES

1. Iida A, Gohshi Y.: Tracer element analysis by X-ray fluorescent. pp307-348 Handbook on Synchrotron Radiation. Vol 4 1991 edited by Ebashi S, Koch M, Rubenstein E. North-Holland, Elsevier Publisher, Amsterdam.
2. Homma S, Sasaki A, Nakai I, Sagai M, Koiso K, Shimojo N. Distribution of copper, selenium, and Zinc in human kidney, tumors by nondestructive synchrotron radiation x-ray fluorescence imaging. J. Trace Elements in Experimental Medicine 6: 163-170, 1993
3. Shimojo N, Homma S, Ohuchi K, Shinyashiki M, Sun GF, Kumagai Y. Mercury dynamics in hair of rats exposed to methylmercury by synchrotron radiation x-ray fluorescence imaging. Life Science 60: 2129-2137, 1997
4. Jonson R, Mattsson S, Unsgaard B.: A method for in vivo analysis of platinum after chemotherapy with cisplatin. Phy. Med. Biol. 33:847-857, 1988
5. Liu N, Zhou C, Yan L, Li X, Chao Z, Ren Z, Zhou S. : A preliminary study on the positional distribution of cisplatin and other elements in the liver of normal mice. Nucl. Instr. Meth. B75:571-575, 1993
6. Homma S, Kumagai Y, Shinyashiki M, Shimojo N. Application of synchrotron radiation x-ray fluorescence imaging combined with histochemical staining to the renal section of mercury-treated rats. J Synchrotron Rad. 5: 57-59, 1998
7. Ektesssabi AM, Rokkum M, Johansson C, Albrektsson T, Sennerby L, Saisho H.Application of synchrotron radiation in investigation of metal-ion release from a hip replacement prosthesis. J. Synchrotron Rad. 5: 1136-1138, 1998
8. Kazama M, Takeda T, Akiba M, Yuasa T, Hyodo K, Ando M, Akatsuka T, Itai Y. Performance study of monochromatic synchrotron x-ray computed tomography using a linear array detector. Med. Imag. Tech. 15: 615-624, 1997
9. Takeda T, Kazama M, Zeniya T, Yuasa T, Akiba M, Uchida A, Hyodo K, Akatsuka T, Ando M, Itai Y. Development of

a monochromatic x-ray computed tomography with synchrotron radiation for functional imaging. Edited by Ando M, Uyama C, Medical Applications of Synchrotron Radiation. pp103-110, Springer-Verlag, Tokyo, 1998

10. Grodzins L. Optimum energies for X-ray transmission tomography of small samples. Application of synchrotron radiation to computed tomography I. Nucl. Instr. Meth. 206: 541-545, 1983
11. Dilmanian FA, Garrett RF, Thomlinson WC, Berman LE, Chapman LD, Gmur NF, Lazarz NM, Luke PN, Moulin HR, Oversluizen T, Slatkin DN, Stojanoff V, Thompson AC, Volkow ND, Zeman HD. Computed tomography with monochromatic x rays from the National Synchrotron Light Source. Nucl. Instr. Meth. B56/57: 1208-1213, 1991
12. Dilmanian FA, Wu XY, Parsons EC, Ren B, Kress J, Button TM, Chapman LD, Coderre JA, Giron F, Greenberg D, Krus DJ, Liang Z, Marcovici S, Petersen MJ, Roque CT, Shleifer M, Slatkin DN, Thomlinson WC, Yamamoto K, Zhong Z. Single- and dual-energy CT with monochromatic synchrotron x-rays. Phys. Med. Biol. 42:371-387, 1997
13. Takeda T, Yu Q, Yuasa T, Hasegawa Y, Yashiro T, Itai Y. Human thyroid specimen imaging by fluorescent x-ray computed tomography with synchrotron radiation. SPIE Proceeding 3772: 258-267, 1999
14. Takeda T, Matsushita S, Wu J, Yu Q, Thet-Thet-Lwin, Zeniya T, Yuasa T, Hyodo K, Dilmanian FA, Akatsuka T, Itai Y: Fluorescent x-ray CT image of rat heart with non-radioactive iodine labeled BMIPP. Proceeding of IEEE-EMBS Asia-Paciffic Conference on Biomedical Engineering: 276-277, 2000
15. Takeda T, Akiba M, Yuasa T, Akatsuka T, Kazama M, Hoshino Y, Hyodo K, Dilmanian FA, Akatsuka T, Itai Y.: Fluorescent x-ray computed tomography with synchrotron radiation using fan collimator. SPIE 2708: 685-695, 1996
16. Takeda T, Maeda T, Yuasa T, Akatsuka T, Ito K, Kishi K, Wu J, Kazama M, Hyodo K, Itai Y.: Fluorescent scanning x-ray tomographic image with monochromatic synchrotron x-ray. Med. Imag. Tech. 14:183-194, 1996
17. Yu Q, Takeda T, Yuasa T, Hasegawa Y, Wu J, Thet-Thet-Lwin, Hyodo K, Dilmanian FA, Itai Y and Akatsuka T. Preliminary experiment of fluorescent X-ray computed tomography to detect dual agents for biological study. J. Synchrotron Rad. 8: 1030-1034, 2001
18. Boisseau P, Grodzins L. Fluorescence tomography using synchrotron radiation. Hyperfine Interactions 33: 283-292, 1987
19. Takeda T, Maeda T, Yuasa T, Akatsuka T, Ito K, Kishi K, Wu J, Kazama M, Hyodo K, Itai Y.: Fluorescent scanning x-ray tomography with synchrotron radiation. Rev. Sci. Instrum. 66(2) :1471-1473, 1995
20. Cesareo R., Mascarenhas S.: A new tomographic device based on the detection of fluorescent X-rays. Nucl. Instr. Meth. A 277: 669-672, 1989
21. Takeda T, Yuasa T, Hosino A et al.: Fluorescent x-ray computed tomography to visualize specific materials distribution. SPIE, 3149: 160-172, 1997
22. Hogan JP., Gonsalves RA., Krieger AS. : Fluorescent computer tomography: A model for correction of X-ray absorption. IEEE Transactions on Nuclear Science 38:1721-1727, 1991
23. Rust GF, Weigelt J.: X-ray fluorescent computed tomography with synchrotron radiation. IEEE Trans.Nucl.Sci. 45: 75-88, 1998
24. Takeda T, Momose A, Yu Q, Yuasa T, Dilmanian FA, Akatsuka T, Itai Y: New types of x-ray computed tomography

with synchrotron radiation: fluorescent x-ray CT and phase-contrast x-ray CT with interferometer. Cellular & Molecular Biology 46: 1077-1088, 2000

25. Takeda T, Yu Q, Yashiro T, Zeniya T, Wu J, Hasegawa Y, Thet-Thet-Lwin, Hyodo K, Yuasa T, Dilmanian FA, Akatsuka T, Itai Y. Iodine imaging in thyroid by fluorescent X-ray CT with 0.05 mm spatial resolution. Nucl. Instr. Meth. in press
26. Simionovici AS, Chukalina M, Drakopoulos M, Snigireva I, Snigirev A, Schroer Ch, Lengeler B, Janssens K, Adams F. X-ray fluorescent microtomography: Experiment and reconstruction. SPIE 3772: 304-310, 1999
27. Schroer Ch, Tummler J, Gunzler TF, Lengeler B, Schroder WH, Kuhn AJ, Simionovici AS, Snigirev A, Snigireva I. Fluorescent microtomography: External Mapping of elements inside biological samples. SPIE 4142: 287-296, 2000
28. Yu Q, Takeda T, Yuasa T, Hasegawa Y, Akatsuka T, Itai Y. Development of high resolution fluorescent x-ray CT with synchrotron radiation. Med. Imag. Tech. 17: 493-494, 1999
29. Yuasa T, Akiba M, Takeda T, Kazama M, Hoshino Y, Watanabe Y, Hyodo K, Dilmanian FA, Akatsuka T, Itai Y.: Reconstruction method for fluorescent x-ray computed tomography by least-squares method using singular value decomposition. IEEE trans. Nucl. Sci. 44:54-62, 1997
30. Hoffer PB, Jones WB, Crawford RB, Beck R, Gottschalk A. Fluorescent thyroid scanning; A new method of imaging the thyroid. Radiology 90: 342-344, 1968
31. LeBlanc AD, Bell RL, Johnson PC. : Measurement of ^{127}I concentration in thyroid tissue by x-ray fluorescence. J. Nucl. Med. 14; 816-819, 1973
32. Patton J. A., Sandler M. P., Partain C. L.: Prediction of benignancy of the solitary Cold thyroid nodule by fluorescent scanning. J. Nucl. Med. 26:461-464, 1985